

The Upscattering of Ultracold Neutrons from the polymer $[C_6H_{12}]_n$

E. I. Sharapov,¹ C. L. Morris,^{2,*} M. Makela,² A. Saunders,² Evan R. Adamek,³ L. J. Broussard,² C. B. Cude-Woods,³ Deion E Fellers,² Peter Geltenbort,⁴ M. Hartl,² S. I. Hasan,⁵ K. P. Hickerson,⁶ G. Hogan,² A. T. Holley,³ C. M. Lavelle,⁷ Chen-Yu Liu,⁸ M. P. Mendenhall,⁶ J. Ortiz,² R. W. Pattie Jr.,⁹ D. G. Phillips II,⁹ J. Ramsey,² D. J. Salvat,³ S. J. Seestrom,² E. Shaw,² Sky Sjue,² W. E. Sondheim,² B. VornDick,⁹ Z. Wang,² T. L. Womack,² A. R. Young,⁹ and B. A. Zeck⁹

¹*Joint Institute for Nuclear Research, 141980, Dubna, Russia*

²*Los Alamos National Laboratory, Los Alamos, NM 87544, USA*

³*Department of Physics, Indiana University, Indiana 47405-7105 USA*

⁴*Institut Laue-Langevin, 38042 Grenoble Cedex 9, France*

⁵*Department of Physics and Astronomy, University of Kentucky, Lexington, Kentucky 40506, USA*

⁶*Kellogg Radiation Laboratory, California Institute of Technology, Pasadena, California 91125, USA.*

⁷*Applied Physics Laboratory, The Johns Hopkins University, Baltimore, Maryland 21218 USA*

⁸*Department of Physics, Indiana University, Indiana 47405-7105 USA*

⁹*Department of Physics, North Carolina State University, Raleigh, North Carolina 27695, USA*

(Dated: August 2, 2013)

It is generally accepted that the main cause of ultracold neutron (UCN) losses in storage traps is the upscattering to the thermal energy range by hydrogen adsorbed on the surface of the trap walls. However, the data on which this conclusion is based are poor and contradictory. Here, we report a measurement, performed at the Los Alamos National Laboratory UCN source, of the average energy of the flux of upscattered neutrons after the interaction of UCN with hydrogen bound in semicrystalline polymer PMP (tradename TPX), $[C_6H_{12}]_n$. Our analysis, performed with the MCNP code based on the application of the neutron scattering law to UCN upscattered by bound hydrogen in semicrystalline polyethylene, $[C_2H_4]_n$, leads us to a flux average energy value of 26 ± 3 meV in contradiction with previously reported experimental values of 10 to 13 meV and in agreement with the theoretical models of neutron heating implemented in the MCNP code.

PACS numbers: 68.49.-h, 78.70.Nx, 68.47.-b

UCN are neutrons with kinetic energy below a critical value of 100 neV (velocity 4.4 m/s). This corresponds to an average temperature of 1 mK, hence the technical term ‘ultra cold’. The UCN neutrons are totally reflected from material surfaces at all angles of incidence and therefore can be confined in traps for time intervals of several hundred seconds – comparable to the neutron lifetime. Recent reviews [1, 2] highlight the use of UCN in nuclear and particle physics, cosmology and gravity. In particular, an importance of study of the upscattering spectrum temperature and rates for neutron lifetime measurements is emphasized in [3]. Authors of Ref. [4] discuss using UCN upscattering techniques in solid state and surfaces studies with the view that the rather limited UCN intensity available at existing UCN sources will be overcome with more powerful next generation UCN sources. For all these studies a better understanding of UCN interactions, especially upscattering, at surfaces of different materials continues to be of importance in a view of existing inconsistencies in data, as detailed in [4]. During the transport in neutron guides or the storage in the material traps, UCN can be excited above the critical energy by absorbing energy from thermal excitation of the surface materials and leave the confinement space. It is presently believed that the main reason for UCN heating in traps is inelastic scattering from the hydrogen molecules on the material surfaces. Indeed, by the nuclear reaction analysis method [5] with ^{15}N beam impinging on the unbaked copper samples, the area density of the surface hydrogen was determined to be 2×10^{16} H/cm² and the hydrogen containing layer was estimated to be 3.0 nm thick.

Hydrogen has one of the largest inelastic scattering cross section of all elements. It is most convenient to study it in polyethylene, $[C_2H_4]_n$, in which the hydrogen inelastic cross section increases as the inverse velocity law to the value of 2053 ± 40 barn [6] at a velocity of 4.0 m/s. Authors of Refs. [7, 8], used a 100- μ m thick polyethylene sample inside a UCN trap and $\sim 4\pi$ 3He neutron detectors of a different gas pressure to observe the upscattered neutron flux and have determined its average energy to be 10-13 meV (the corresponding velocity ~ 1600 m/s). This is about half of the value expected from the known phonon frequency spectrum of hydrogen in polyethylene, and has triggered further efforts to find possible channels of the UCN escaping from traps. Authors of Ref. [9], using the neutron activation method, searched for lower energy upscattering of UCN from a Be

*Corresponding author; Electronic address: morris@lanl.gov

surface. A possibility of scattering in the range of 15 to 300 m/s was convincingly ruled out. Also, so called "weak heating" with UCN energy changes $\simeq 10$ neV above the critical energy has been reported [10], with a probability estimated to be $\sim 10^{-7}$ per the collision with copper, which is rather low value. In this report we study UCN upscattering into the thermal energy range in polymethylpentene (PMP), $[\text{C}_6\text{H}_{12}]_n$, which, due to its low density (0.83 g/cm^3), is a material having negative, practically non-reflective optical potential U_F with the value even smaller than U_F for a more often used polyethylene (PE), $[\text{C}_2\text{H}_4]_n$. Our PMP (tradename TPX, Mitsui Chemicals, Inc. for the atactic poly[4-methyl-1-pentene] material) was a tetragonal of Form I semicrystalline sample with XRD spectrum similar to that of the undrawn sample in [11] as was evidenced by our own X-ray diffraction data.

The measurements have been performed at the Los Alamos National Laboratory solid-deuterium ultracold neutron source driven by the 800 MeV, $5.8\text{-}\mu\text{A}$ average proton beam provided by the Los Alamos Neutron Science Center (LANSCE) linear accelerator. The source is described in details in a recent publication by Saunders et al. [12]. The scheme of the experimental geometry is shown in Fig. 1. A 7.62 cm diameter stainless steel UCN guide tube (1) was connected to the main UCN guide through the section containing a flange with a zirconium foil embedded in the 6 T field of a superconducting solenoid magnet. This Zr foil separates the UCN source vacuum system from the external guide. The magnetic field accelerates half of the neutrons above the foils critical energy allowing the high field seaking beam to exit the UCN source, reducing losses due to transmission through the foil. The 500 μm thick PMP sample (2) with the same diameter as the inside of the tube was installed at the end of the shown section. The density of the UCN beam in the tube was $\simeq 1.0 \text{ UCN/cm}^3$, and the average velocity of the UCN flux spectrum was $\simeq 4 \text{ m/s}$. Two 5 cm diameter, 30 cm long, drift tube ^3He neutron detectors (3) and (4) were installed perpendicular to the guide axis and symmetrically above and below it, as shown in Figure 1, to provide equal fluxes for both detectors. The construction, gas filling and performance of detectors are described in [13]. The partial ^3He pressure was 1.8 bar in one detector and 0.2 bar in the other one. Data were accumulated for 300 sec under steady beam conditions. The up-scattered neutron rates were significantly above the background, which was mostly due to cosmogenic thermal neutrons. The background associated with the proton beam was eliminated using time gates on the analog to digital converters, to reject events during the beam pulses. The neutron rates for the analysis were calculated by integrating the measured pulse height spectra from both detectors. The ratio $R = N_{1.8}/N_{0.2}$ of integrated rates was compared with calculations to deduce the average energy $\langle E \rangle$ of the upscattered flux. Data were also taken with a 6.3 mm thick polyethylene slab inserted between detectors and the end of the UCN guide to thermalize completely the upscattered neutrons and to compare the result with calculations.

In principle, if the scattered flux has Maxwellian shape, the flux average energy $\langle E \rangle$ can be easily estimated following the following argument. The efficiencies ϵ of the ^3He detectors for neutron with energy E crossing the tubes along the same track ℓ are different because $\epsilon = 1 - \exp\{-N(^3\text{He})\ell\sigma(E)\}$ while the Helium-3 atomic densities $N(^3\text{He})$ are different for the 1.8 bar and 0.2 bar detectors ($\sigma(E)$ is well known cross section for the $^3\text{He}(n,p)\text{T}$ reaction). We calculated efficiencies for several Maxwellian spectra with different $\langle E \rangle$ using the code MCNP5 [14] to follow all neutron trajectories crossing our detectors in the geometry of Fig. 1. A calculation of R vs. $\langle E \rangle$ (shown in fig. 2) provides then the average energy of the Maxwellian upscattered spectrum using the measured value of R . However, Maxwellian shape for the upscattered flux is not expected from the theory of neutron inelastic scattering by a bond hydrogen.

For UCN upscattering, a simple analytical formula for the isotropic differential cross section in one-phonon incoherent approximation of the theory

$$\frac{d\sigma_{up}}{dE} = \sigma_b \sqrt{\frac{E}{E_i}} \left(e^{E/kT} - 1 \right)^{-1} \frac{g(E)}{A} e^{-2W} \quad (1)$$

demonstrates clearly that the upscattering spectrum is not Maxwellian. This equation, written initially in terms of the neutron wave vector variable, was obtained by Placzek and Van Hove [15]. Here $\sigma_b = 4\pi b^2$ is the cross section for bound nuclei with the mass number A , E_i is the initial UCN energy, E is the energy after upscattering, $g(E)$ is the generalized (amplitude weighted) phonon density of states in the material under study and the last exponent is the material- and temperature-dependent Debye-Waller factor. At a temperature of 300K, multi-phonon contributions are also important [16] and a full upscattering spectrum is often calculated then with the use of the MCNP code and its models for the neutron scattering law $S(\alpha, \beta)$ [17] (α and β are neutron reduced momentum and energy transfers) which takes some account for multiphonon processes. The issue of different theoretical approaches to multiphonon scattering is of interest itself but we leave it out of the present report because our experimental data can't distinguish between them. A most recent model of the generalized density of states of hydrogen in PE is provided by Barrera et al. [18]. It was validated recently by neutron inelastic measurements [19] for the high density PE. Using these data and the deduced $S(\alpha, \beta)$ one of the authors (C.M.L.) created the 77K and 293K scattering kernels, represented as tables of the double differential scattering cross sections for modeling the neutron

transport in PE. Although such data are absent for the polymer PMP, we believe that its neutron scattering law is similar to the $S(\alpha, \beta)$ of PE and one can use PE as a model for UCN upscattering from PMP. Indeed, the known experimental infrared spectra are similar for PMP [20] and PE [21] and the same is valid for numerous theoretical calculations, as referenced for example in [22]. Of course, the presence of the methyl groups in the side branches of the PMP molecular chain can additionally influence the low energy range of PMP phonon density of states, not accessible in infrared and Raman spectroscopy, and we address this issue in the concluding paragraph.

Therefore, with the PE new kernels added to the MCNP thermal energy data we modeled the scattered flux from our PMP sample in the experimental geometry of Fig. 1 with an initial neutron beam energy $E_{in} = 100$ neV. The results are shown in Fig. 3. The shape of the directly upscattered flux (black squares) is clearly not Maxwellian and was found to be independent of the initial neutron energy and the placement of detectors. The spectrum of the fully moderated (by the additional 6.3-mm thick polyethylene slab placed between the sample and detectors) flux is Maxwellian. Having proved these spectral shapes we modeled the ${}^3\text{He}(n,p)\text{T}$ reaction rates in the two detectors after the UCN scattering using the 293K kernel. The results of modeling together with the results of measurements are presented in TABLE I for comparison.

TABLE I: Experimental results in comparison with the MCNP-modeling. N(1.8) and N(0.2) represent count rates taken during the 300 s run with detectors of the 1.8 bar and 0.2 bar ${}^3\text{He}$ pressure. R(exp) and R(mcnp) represent their ratios.

Neutron spectrum	N(1.8)	N(0.2)	R(exp)	R(mcnp)
Upscattered	71159	14943	4.76 ± 0.07	4.67
Moderated	32360	5264	6.14 ± 0.09	5.90
DOUBLE RATIO			0.77 ± 0.02	0.79

As shown in TABLE I, the measurements on the PMP sample and the MCNP modeling with the use of the PE 293K kernel based on theoretical $S(\alpha, \beta)$ scattering law agree rather well. In the modeling, the non-Maxwellian scattered spectrum for a thin sample has the average energy value of 26 ± 3 meV. Therefore we conclude that, after the initial UCN energy, the spectrum of neutrons, scattered in one or only few interactions, has the expected non-Maxwellian shape and the average energy $\langle E \rangle = 26 \pm 3$ meV. At the same time, the fully moderated flux spectrum has Maxwellian shape with the average energy of 53 ± 4 meV at room temperature. Our conclusion contradicts obviously with the value $\langle E \rangle = 10 - 13$ meV [7, 8], obtained in an essentially the same kind of the experiment although with a different ${}^3\text{He}$ detector, with a PE sample and by the analysis in a frame of Maxwellian approximation. This situation induced us to reanalyze data [7, 8] using the MCNP code with the input describing geometry and conditions of the measurement [8]. The result is shown in Fig. 4, where the full squares are experimental data of [8] and curves 1 and 2 have been obtained by the MCNP modeling with the scattering law $S(\alpha, \beta)$ kernels at 77K and 293K to produce non-Maxwellian theoretical spectra with $\langle E \rangle = 11$ meV and $\langle E \rangle = 26$ meV, correspondingly. The curve 3 for the 293K Maxwellian spectrum is shown for comparison. From agreement of experimental data with the curve 2 we claim the average energy of 26 meV in the PE experiment of Stoika and Strelkov [8] – the same average energy as in our PMP experiment modeled with the neutron scattering law $S(\alpha, \beta)$ for PE.

This comparison of two experiments allows us to conclude that, as suggested in the text of this report, the phonon densities of states in polyethylene and polymethylpentene are similar. Finding possible low energy distinctions between them would require dedicated UCN and thermal neutron inelastic scattering measurements.

Acknowledgment We thank L. Daemon for help in acquiring X-ray diffraction data for our samples. This work was performed under the auspices of the U.S. Department of Energy under Contract DE-AC52-06NA25396. Author DJS is supported by the DOE Office of Science Graduate Fellowship Program, made possible in part by the American Recovery and Reinvestment Act of 2009, administered by ORISE-ORAU under Contract DE-AC05-06OR23100.

[1] W. Michael Snow, *Physics Today* **66**(3), 50 (2013).

[2] S. K. Lamoreaux and R. Golub, *J. Phys. G: Nucl. Part. Phys.* **36**, 104002 (2009).

[3] R. Picker et al., *Nuclear Instruments and Methods in Physics Research A* **611**, 297 (2009).

[4] E. Korobkina and R. Golub, *J. Butterworth and P. Geltenbort, S. Arzumanov, Phys. Rev. B* **70**, 035409 (2004).

- [5] W. A. Landford, R. Golub, Phys. Rev. Lett. **39**, 1509 (1977).
- [6] Yu. N. Pokotilovski, M. I. Novopoltsev, P. Geltenbort, and T. Brenner, Instruments and Experimental Techniques, **54**,16 (2011).
- [7] A. D. Stoika and A. V. Strelkov, M. Hetzelt, Z. Physik B **29**, 349 (1978).
- [8] A. D. Stoika, A. V. Strelkov, P3-11593, Communications of the Joint Institute for Nuclear Research, Dubna, 1978.
- [9] Al. Yu. Muzhichka and Yu. N. Pokotilovski, P. Geltenbort, Journal of Experimental and Theoretical Physics, **88**, 79 (1999).
- [10] A. V. Strelkov, V. V. Nesvizhevsky, P. Geltenbort et al., Nuclear Instruments and Methods in Physics Research A **440**, 695 (2000).
- [11] Tianbei He and Roger S. Porter, Polymer **28**, 1321 (1987).
- [12] A. Saunders, M. Makela, Y. Bagdasarova et al., Review of Scientific Instruments **84**, 013304 (2013).
- [13] Zhehui Wang, C. L. Morris, M. Makela et al., Nuclear Instruments and Methods in Physics Research A **605**, 430 (2009).
- [14] X-5-Monte-Carlo-team, MCNP – a General Monte Carlo N-Particle Transport Code, Version 5, Report No. LA-UR-03-198, Los Alamos National Laboratory, Los Alamos, 2003.
- [15] G. Placzek and L. Van Hove, Phys. Rev. **93**, 1207 (1954).
- [16] T. Kitagawa and T. Miyazawa, Polymer Letters **6**, 83 (1968).
- [17] R. E. MacFarlane, *Neutron Slowing Down and Thermalization*, in: *Handbook of Neutron Engineering*, pages 189-277 (Springer Science and Business Media, USA, 2010).
- [18] G. D. Barrera, S. F. Parker and A.J. Ramirez-Cuesta, P. C. H. Mitchell, Macromolecules **39**, 2683 (2006).
- [19] C. M. Lavelle, C.-Y. Liu, M. B. Stone, Nuclear Instruments and Methods in Physics Research A **711**, 166 (2013).
- [20] SIGMA-ALDRICH LLC, //www.sigmaaldrich.com/spectra/rair/RAIR003202.PDF (2013).
- [21] S. Krimm, C.Y. Liang, and G. B. B. Sutherland, Journal of Chemical Physics A **25**, 549 (1956).
- [22] A. Kumar et al., Macromol. Symp. **277**, 51 (2009).

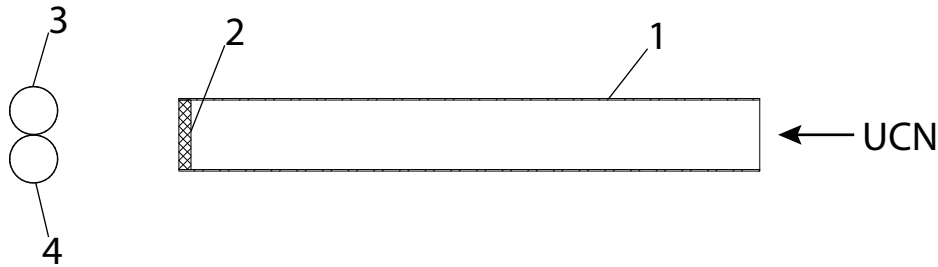


FIG. 1: Scheme of a section of the neutron guide and the drift-tube detectors placement for measuring upscattering of ultracold neutrons: 1) is the neutron guide, 2) is the sample, and 3) and 4) are the neutron detectors.

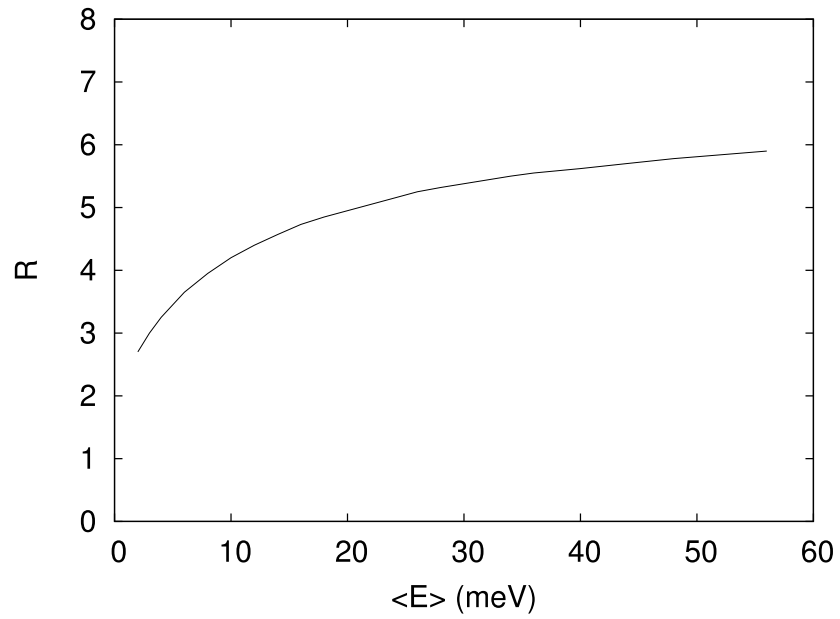


FIG. 2: The calculated ratio R of the LANL drift-tubes (with the 1.8 and 0.2 bar of He-3 partial pressure) efficiencies versus the average energy $\langle E \rangle$ of the Maxwellian scattered flux. It would give the result for $\langle E \rangle$ from measured R if the assumption of the Maxwellian shape for the neutron flux is valid. As explained in text we do not use this assumption in analyzing our data.

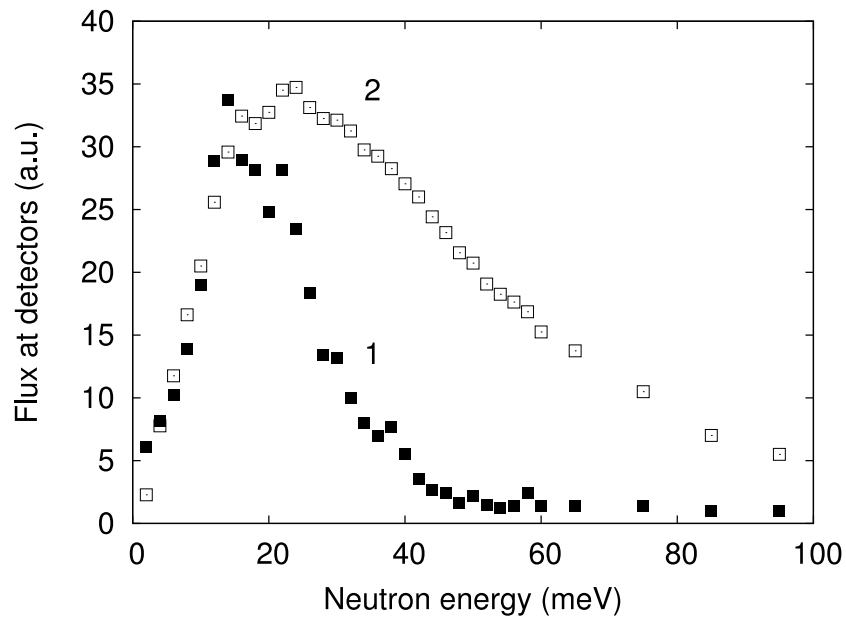


FIG. 3: The calculated energy spectra of the neutron flux scattered from the PE sample, $500 \mu\text{m}$ thick, $E_{in}=100 \text{ neV}$ (curve 1), and of the fully moderated flux (curve 2) after "filtering" this flux through the 6-mm polyethylene slab. The spectra are obtained by MCNP modeling with the 293K $S(\alpha, \beta)$ scattering law. The shape of spectrum '1' is not Maxwellian, it has the average energy value of $26 \pm 3 \text{ meV}$. Spectrum 2 is a Maxwellian with the average energy of $53 \pm 4 \text{ meV}$.

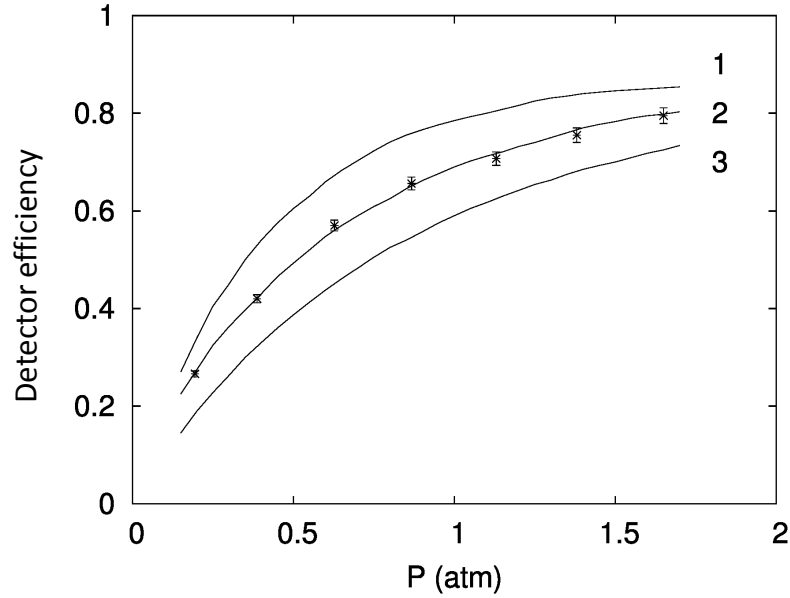


FIG. 4: Reanalysis of the Stoika and Strelkov [8] PE experiment. Experimental data [8] for their neutron detector efficiencies as a function of the He-3 pressure are shown as crosses. Curves 1 and 2 – show our MCNP modeling of their detector efficiencies, which we performed using the PE scattering law $S(\alpha, \beta)$ kernels at 77K and 293K. Curve 1 corresponds to non-Maxwellian upscattered spectrum with $\langle E \rangle = 11$ meV, for getting which we resorted to the 77K kernel. Curve 2 corresponds to the 293K spectrum with $\langle E \rangle = 26$ meV. Curve 3 for the 293K Maxwellian spectrum is shown, following [8], for comparison. From agreement of data [8] with the curve 2 we deduce the average energy of 26 meV for their PE experiment, which is the same as the result of our PMP experiment.